Process design of Synthetic Natural Gas (SNG) production using wood gasification

Alexis Duret, Claude Friedli, François Maréchal*

Swiss Federal Institute of Technology, Lausanne, CH-1015 Lausanne, Switzerland

Abstract

The process design of a 10 to 20MW_{th} Synthetic Natural Gas (SNG) production process from wood has been performed. Combining process modeling and process integration techniques, this study proceeds via the following stages:

- thermodynamic modeling: mass, energy balances and simulation of the wood gasification, the methanation and the purification units;
- process integration that identifies the energy saving opportunities and prepares a thermo economic optimization.

This work demonstrates that the process can transform wood into pipeline quality methane with a thermal efficiency of 57.9% based on the Lower Heating Value (LHV). The process integration study shows that the heat surplus of the process can be used to almost satisfy the mechanical work required by the process; only 7% of the mechanical needs should come from an external source.

Keyword: bioenergy, gasification, wood to methane, methanation, process design, process integration

Introduction

The world wide energy consumption is constantly increasing and it will certainly still increase during at least the 21st century [1]. Currently, the major part of this consumption is satisfied by fossil fuels (87% of the world primary energy consumption [2]). Since, a limited amount of these fuels are available and since these fuels are responsible for the majority of the greenhouse gas emission, it is really important to find new sustainable energy sources able to replace fossil fuels. Unfortunately most of the renewable energy sources suffer from several drawbacks: they are not available in sufficient quantity, they are stochastically distributed in the world and they are difficult to store. Furthermore, unless converted into electricity, they do not benefit from an existing distribution network.

Biomass and especially wood represent an exception: they may be converted and distributed as bio-gas or bio-fuels, the combustion of which emits only a small amount of NO_x and SO_x. In Switzerland, the amount of wood available is sufficiently important to considerably reduce the CO_2 emissions [3].

*Corresponding author: FAX: 0041216933502, email: francois.marechal@epfl.ch

In this context, a project called *From Wood to Methane* [4] has been launched in Switzerland; it involves several academic institutes (the Paul Scherrer Institute, PSI, the Ecole Polytechnique Fédérale de Lausanne, EPFL and the Swiss Federal Laboratories for Materials Testing and Research, EMPA) and one private partner (*GAZObois* SA). The aim of this project is to develop a 10 to 20 MW_{th} semi industrial plant to produce SNG from wood whose quality matches that of natural gas thus allowing its direct injection in the high pressure Swiss natural gas network.

The objective of the work presented here is to perform a preliminary study of the process design in order to find its optimal operating parameters. The methodology used here combines process modeling and process integration techniques. It proceeds through two steps:

- first a thermodynamic model of the process is built;
- then a process integration identifies the energy saving opportunities and prepares the thermo economic optimization.

The conversion chain leading from wood to SNG proceeds through three steps. Wood is first gasified into a mixture mostly made of hydrogen (H_2), carbon monoxide (CO), carbon dioxide (CO_2) and methane (CH_4). This syngas is then further converted in a catalyzed methanation reactor and the final methane rich gas is purified. The first step of the process is endothermic, the second is exothermic while the third is approximately neutral in terms of heat. The process design and integration will therefore play a major role in the performances of the whole conversion process.

Modeling the process

The models presented in this work have been built using a process simulation commercial software (BELSIM-VALI[5]) using an equation oriented solving procedure that has been used for data reconciliation as well as for process design purposes. In our application, the interest of such a tool is mainly due to its versatility with respect to the set of specifications: when dealing with data reconciliation from experiments or when performing parameter identification, process modeling or optimization, the same process structure and the same solving procedure can be used.

The process flow sheets developed for this study are presented on figures 2, 3 and 4. Each of the three steps of the conversion from wood to methane is described in more details below.

Step 1: Gasification

The wood gasification is performed using a Fast Internally Circulated Bed reactor (FICFB), an indirect fluidized bed reactor [6] (figure 1). This reactor features several advantages: *(i)* the flexibility of the heat source, *(ii)* it produces a high purity gas (almost free of nitrogen) without having to use pure oxygen as oxidizing agent, and *(iii)* it produces a gas with a high heating value.

The basic idea of the FICFB reactor consists in the separation of the fuidized bed in two zones:

*Corresponding author: FAX: 0041216933502, email: francois.marechal@epfl.ch

- a combustion zone, fluidized with air, in which wood residues are burned to heat the bed material up to 850–900°C;
- a gasification zone, fluidized with steam, in which the biomass is converted to syngas using the heat carried by the circulating bed material; the temperature of this zone ranges typically from 750°C to 800°C.

A 8 MW_{th} input demonstration plant based on this FICFB reactor has been built in Güssing (Austria) and started up in 2002 [7]. At present time, this pilot plant is coupled with a gas engine to produce up to 2 MW_{el} and 4.5 MW_{th} for district heating. The first law global efficiency of the whole system corresponds to about 80% of the wood Lower Heating Value (LHV).

From the thermo-chemical point of view, the wood gasification process can be divided in three phases [8]:

- in phase 1, the volatile compounds contained in the biomass are vaporized (pyrolysis); at the end of this step the product obtained is a gas containing high molecular weight hydrocarbons (oil, naphta and tar: mainly condensable organic compounds) and charcoal (compound richer in carbon than the biomass, usually called *char*);
- in phase 2, the volatile compounds produced during phase 1 are either cracked or reformed by steam in lower molecular weight compounds;
- during phase 3, charcoal is partly gasified by gasifying agents (oxygen or steam) through heterogeneous reactions (gas-char reactions); homogeneous reactions may happen simultaneously in the gas phase leading to the final product of the gasification. Table 1 gives a non-exhaustive list of these reactions and the related thermodynamic data [8].

Figure 2 presents the flow chart of the model developed for the gasification step. The main steps of the model are the following: first biomass (*BIOMASS*) and 12bar steam (*STEAM*) are injected in the gasification zone (*PYROL*) where the wood is decomposed into a solid phase and syngas. The lower heating value of the biomass dry and free of ash (LHV_{daf}) is 18,2 MJ/kg. The outlet stream (*F*) of the gasification zone contains a solid phase and a gas phase. The solid residue is separated from the product gas in *SEPSG*; it represents the char that remains in the fluidized bed and that will be transferred to the combustion zone. In the model, it is assumed that the wood conversion into char is a constant that will be identified using the heat balance and experimental data obtained with the FICFB pilot plant. The gas stream (*SYNGAS*) is then cooled down to 25°C in the heat exchanger *E-1*. The water contained in this stream is condensed and separated from the gas phase in *DRYING1*. The dry gas obtained is then desulfurized in *H2SREM* (adsorption on a ZnO column [15]). The clean gas (*SYNCLEAN*) is then divided (*S-1*) into two streams: *RESYN* serves as supplementary fuel in the combustion zone *R-2* and *SYNG* leaves the process and enters the methanation step (Fig. 3).

The solid residue (*CAR*) leaving *SEPSG* is injected with a part of the syngas produced (RESYN) in the combustion zone *R-2* where they are burned with compressed air (*AIRP*). This solid residue is considered to be pure carbon. The combustion in *R-2* is

*Corresponding author: FAX: 0041216933502, email: francois.marechal@epfl.ch

assumed to be stœchiometric and adiabatic. The hot gases (*FUME*) leaving the combustion zone are cooled down in the heat exchanger *E-2* from the adiabatic temperature of combustion to the temperature of the gasification zone plus 100°C, temperature difference of the circulating bed material between the combustion zone and the gasification zone. The heat recovered (*q-2*) in this heat exchanger represents the heat transferred from the combustion to the gasification zone by the circulating fluidized bed material; it is assumed to satisfy the heat requirement of the gasification zone and to complement its heat loss (10% of the heat demand). The combustion gases are finally cooled to 150°C in a second heat exchanger *E-3*. The process integration analysis will define the waste heat recovery process structure.

The modeling approach has been designed in two phases: *(i)* first a data reconciliation of the pilot plant data is performed to compute performance parameter; *(ii)* finally, by fixing these parameters, we are able to simulate the behavior of the gasification reactor.

In order to determine the number of independent chemical reactions that have to be considered in the gasification zone, the number of degree of freedom around this zone must be known. It can be determined as follow. The concentration of nine species must be calculated (Table 5) in the outlet stream (*F*). A heat balance and four atomic mass balances reduce this number to five. Moreover, it is assumed that the wood is completely converted into char and syngas in the gasification zone. Finally, the solid phase flow rate in stream *F* can be calculated using the hypothesis that the heat produced in the combustion zone satisfies the heat required by the gasification zone. These considerations allow reducing the degree of freedom of the gasification zone to three. Therefore three reactions (1.4), (1.5) and (1.7) with ethylene, n=2, m=4, are considered in the gasification zone (see Table 1). Only homogeneous reactions have been chosen since the gas phase is more likely to reach the thermodynamic equilibrium than the solid state.

In a first run, the assumption is made that the homogeneous reactions (1.4), (1.5) and (1.7) occurring in the FICFB gasification zone are governed by their thermodynamic equilibrium constant calculated at the gasification temperature. Consequently, the gas phase of stream *F* is at its thermodynamic equilibrium. An expression of the thermodynamic equilibrium constant $K_{P,r}$ of a homogeneous gas phase reaction *r* is given by equation (1) [9]:

$$K_{P,r}(T) = K_r(T)P^{\Delta\nu_r} = \prod_i (Py_i)^{\nu_{i,r}} = e^{\frac{-\Delta_r G^0_{T,r}}{RT}} \qquad (1)$$

where y_i is the molar fractions of compound *i*, $\nu_{i,r}$ the stoichiometric coefficients of compound *i* in reaction *r* and $\Delta_r G^0_{T,r}$ the Gibbs energy of reaction r at temperature T and at standard pressure.

The Gibbs energy of the reaction r at temperature T is given in equation (2a). This thermodynamic function can be expressed as a function of the enthalpy of the reaction (equ. 2b) and the entropy of the reaction (equ. 2c).

*Corresponding author: FAX: 0041216933502, email: francois.marechal@epfl.ch

$$\Delta_r G^{\theta}_{T,r} = \Delta_r H_T - T\Delta_r S_T \quad (2a)$$

$$\Delta_r H_T = \Delta_r H^{\theta}_{T_0} + \int_{T_0}^{T} \Delta_r Cp(T)dT \quad (2b)$$

$$\Delta_r S_T = \Delta_r S^{\theta}_{T_0} + \int_{T_0}^{T} \frac{\Delta_r Cp(T)}{T} dT \quad (2c)$$

where $\Delta_r C_P = \sum_i \nu_{i,r} C_{P,i}$

$C_{P,i}$ being the heat capacity of the compound i at constant pressure.

Combining equations 2a, 2b and 2c, the thermodynamic equilibrium constant and consequently the gas mixture composition can be formulated as a function of the temperature.
The model of the Güssing pilot plant based on the thermodynamic assumption exhibits a behavior similar than the model presented by Schuster et al. [10] based on the same assumption. A comparison of the experimental data with the results obtained using this model shows that the wood gasification process is not completely governed by thermodynamic equilibrium.
Therefore the temperatures associated with each of the three reactions used in the gasification zone have been independently varied in order to fit the experimental data available from the demonstration plant. A new expression of the thermodynamic equilibrium constant for reaction r is given by equation (3):

$$\prod_i (Py_i)^{\nu_{i,r}} = e^{\frac{-\Delta_r G_{T+\Delta T_r}}{R(T+\Delta T_r)}} \quad (3)$$

Where ΔT_r corresponds to the difference between the thermodynamic equilibrium temperature of reaction r and the gasification temperature. By varying ΔT_r, it is possible to find a temperature at which the thermodynamic equilibrium constant is equal to the partial pressure product of equation (3) obtained experimentally. This allows modeling the kinetic effects in a simple way while satisfying the real heat and mass balance. In our approach, the data reconciliation procedure has been used to compute the char to wood inlet ratio and ΔT_r for each of the three reactions considered in the gasification zone. These parameters will be considered as constant in the simulation model.

Step 2: Methanation

The gas mixture entering the methanation process is mainly composed of H_2, CO, CO_2 and CH_4.

Following the reversible reactions given in table 2, the concentration of CH_4 is increased during the methanation. The three first reactions are highly exothermic: they are thus favored by low temperature, unlike reaction (2.4). All four reactions are also favored (or insensitive to) by a high pressure, because of their positive stoichiometric

*Corresponding author: FAX: 0041216933502, email: francois.marechal@epfl.ch

variations. Finally, reaction (2.4) shows that a minimum amount of steam is required to reform the ethylene.

The main problem to be addressed while designing a methanation process of a CO/H2 gas mixture is the control of the temperature in the reactor by an efficient heat transfer system. Most of the processes solve this problem by simply performing the methanation in successive adiabatic units and/or by diluting the gas mixture through recycling loops (Lurgi [12], Hygas [13]). The *Comflux* process [14], designed by Thyssengas in the 80's is an exception. It is based on a pressurized fluidized bed reactor with an internal cooling system which allows performing an isothermal once through methanation of coal gas.

The results [15] obtained with a pilot plant designed to produce 2000 Nm^3/h at 60 bar of SNG from coal syngas are reported in the literature. Operated from 1980 until 1985 during 8000 hours, the plant produced 11 millions Nm^3 of SNG and 16000 tons of superheated steam (120 bar and 420°C). The concentration of CH_4 in the syngas was high enough to meet the pipeline quality requirement without CO_2 removal. This is due to the fact that the H_2/CO ratio, adjusted to lie between 2.7 and 4, was close to the reaction stochiometry; consequently only a small amount of CO_2 was produced by the water gas shift reaction. The advantages of the *Comflux* process are numerous: *(i)* it can be operated at high temperature while keeping a good conversion efficiency of the CO/H_2 mixture since the methanation is done at high pressure; *(ii)* the heat of the exothermic methanation reaction can be used to produce high-pressure super heated steam (excellent valorization of the heat of the reaction); *(iii)* a large flow rate of gas mixture can reacted in a relatively small reactor due to the high operating pressure; *(iv)* the temperature inside the fluidized bed reactor can be well controlled by the internal cooling system and a recycling loop, and finally *(v)* the report [15] shows that the process is reliable and can be scaled up. The only major disadvantage of this process is the important quantity of gas that have to be compressed before the injection in the conversion reactor, requiring thus a large amount of mechanical work.

That is the reason why a *Comflux* configuration has been chosen here. The model developed for the methanation process is presented in figure 3. The main steps of this model are the following: first the biogas from the gasification unit (*SYNG*) is pressurized (*C-1R*) to the methanation reactor pressure (60 bar). It is then preheated (*E-3R*) and mixed (*B-2R*) with the two gas mixtures coming from the two recycling loops (*CH4RE1* and *RECY2*). The stream obtained (*MIX2*) is mixed (*B-3R*) with hot pressurized water at 200°C and 60 bar (*H2OH*). Then this mixture (*MIX3*) is injected in the fluidized bed reactor (*METHANR*) where the methanation reactions (2.1) and (2.2) take place. Only two independent chemical reactions are needed to calculate the composition of the outlet stream of the reactor since there are only seven chemical species in this stream.

The heat (*q-MR*) is removed from the methanation reactor to maintain the reactor at the desired temperature. The gas produced (*CH4H*) is then cooled down (*E-5R*) to 30°C. The condensed water (*H2OOUT*) during this phase is separated (*F-1R*) from the gas mixture (*CH4DR1*). Part of the gas obtained (*RECY1*) goes back to the beginning of the process after compression to 60 bar. The remaining part (*CH4DR2*) leaves the process as a mixture of mostly carbon dioxide and methane and enters the

*Corresponding author: FAX: 0041216933502, email: francois.marechal@epfl.ch

purification step. The condensed water (*H2OOUT*) still contains a lot of methane (7-10 mol%) because of the relative high pressure (50 bar). The report on the *Comflux* pilot plant [15] does not mention the quantity of methane that is lost in this stream. Two alternative procedures have been evaluated to recover this methane. In the first one, the stream of water loaded with dissolved methane (*H2OOUT*) is flashed adiabatically in a valve (*V-1R*) from 50 to around 19 bar. The liquid/gas mixture (*H2OOUT1*) coming out from this valve is separated in the flash drum *F-2R* as a liquid stream (*H2OOUT2*) with a low content of methane (2-4 mo%l) which leaves the process, and a gas stream rich in methane and carbon dioxide (*CH4RE*) which is recycled after compression to 60 bar (*C-3R*). In the second alternative (not described here), the gas stream *CH4RE* is burnt in order to produce heat.

The model for the methanation step was run using the assumption that all the reactions taking place in the *Comflux* reactor were at their thermodynamic equilibrium. Due to a lack of coherent experimental measurements in [15], it has not been possible to validate this assumption on the comflux model described above.

However, this hypothesis has been validated by modeling the fluidized bed methanation reactor from the LEM-PSI [16]. Data reconciliation calculation has shown that the difference of temperature between the thermodynamic equilibrium and the measured temperature needed to fit the experimental data were close to zero for each reaction considered in the methanation reactor (table 2)

Step 3: Gas purification

The gas mixture obtained at the end of the methanation (*CH4DR2*) is mainly composed of CO_2 (45.9 %vol.) and CH_4 (47.6 %vol.). The average composition of the natural gas in the Swiss natural gas network is 91.9% CH_4, 3.7% C_2H_6 and 1% C_3H_8. In order to inject the SNG into the Swiss high pressure network, it must have the following properties: *(i)* a dew point smaller than –12°C at 70bar which corresponds to a water concentration of less than 50 mg/Nm^3 that prevents the formation of hydrate; *(ii)* a Wobbe index ($W_{s,n}$) between 13.3 and 15.7 kWh/Nm^3; equation (4) is used to calculate this index:

$$W_{s,n} = \frac{LHV}{\sqrt{d}} \qquad (4)$$

where d is the specific density of the gas, and *(iii)* a sulfur content below 5 mg/Nm^3.

CH4DR2 needs thus a purification to meet the pipeline quality requirements. Basically, this step should remove as much CO_2 as possible without a significant loss of CH_4, the final concentration of CH_4 being of at least 90%. Moreover, this purification step should have a low specific energy consumption. It should also be able to operate under high pressure since the pressure of the gas mixture coming out of the methanation is about 50-60 bar. According to all the requirements listed above, a process combining three membranes has been chosen. This simple purification method is often used to clean landfill gas [17] which composition is similar to that considered here. It shows the advantage of consuming a small amount of energy per Nm^3 of gas treated. It can be operated at high pressure and with a typical recovery

*Corresponding author: FAX: 0041216933502, email: francois.marechal@epfl.ch

efficiency of CH_4 of 95 %. Finally, membranes with high CO_2/CH_4 selectivity as high as 30 to 35 are available [18].

The flow diagram of this process is shown in figure 4. The compressed, dry and desulfurized gas (*CH4DR2*) is first injected in membrane 1 (*M1M*) where it is partially enriched in methane. The retention stream (*RET1*), already rich in CH_4, is injected in a second membrane (*M3M*) where it is enriched again to its final composition (*SNG*). To avoid an excessive loss of CH_4, the corresponding permeation streams, rich in CO_2 (*PERM1* and *PERM3*) are mixed together, compressed and injected in a third membrane (*M2M*). The permeation stream (*PERM2*) coming out of this membrane leaves the process, while the retention stream rich in CH_4 (*RECY*) returns to the inlet of the gas purification.

To calculate the compositions and the flow rates of the retention and the permeation streams for the binary gas mixture, two equations are needed:

- the definition of the recovery ratio of methane, θ_A :

$$\theta_A = \frac{x_{AR} R}{x_{AF} F} \tag{5}$$

where x_{AR} and x_{AF} are the molar fractions of methane in the retention and in the feed streams respectively and F and R are respectively the flow rates of the feed and the retention streams;

- the definition of the selectivity of methane over carbon dioxide, $\alpha\,(A/B)$ is given by equation (6):

$$\frac{x_{AP}}{1-x_{AP}} = \alpha(A/B)\frac{x_{AR}-\frac{P_P}{P_F}x_{AP}}{(1-x_{AR})\frac{P_P}{P_F}} \tag{6}$$

where x_{AP} and x_{AR} are respectively the molar fractions of methane in the permeation and in the retention streams, P_F the feed pressure and P_P the permeation stream pressure.

For a given selectivity, the concentration of methane in the retention stream is a function of its recovery ratio: the higher the recovery ratio, the lower the concentration of A in the retention stream and the lower the loss of A in the permeation stream.

Process integration

The models described in the three previous steps have been combined to build a model leading from wood to methane. Table 3 gives the composition and the flow rates of the inlet streams of the process. For wood, this flow rate corresponds to a 20 MW_{th} plant, as calculated with a LHV_{daf} for wood of 18.2 MJ kg^{-1}.

Process integration techniques are used to model the heat exchanger network and to compute optimal integration of combined heat and power production [19].

*Corresponding author: FAX: 0041216933502, email: francois.marechal@epfl.ch

Results and discussion

Step 1: Gasification

Table 4 summarizes the model hypothesis made for each unit of the gasification process. For the data reconciliation calculation based on the experimental data from the Güssing pilot plant, the following experimental errors have been considered for each available measurement: ± 0.1 bar on pressures, ± 5 K on temperatures, ± 20% on flow rates, ± 20% on compositions of the outlet gas, and ± 10% on heat losses in the gasification zone and on the rate of syngas recycling.

Table 5 presents the composition of the inlet streams and compares the results of the modeling with the experimental measurements. Table 6 gives the difference between the thermodynamic equilibrium temperature and the measured temperature (ΔTr) for each chemical reaction occurring in the gasification zone found after the data reconciliation calculation. These differences are really important, especially for the methane decomposition reaction (1.4). This means that the reactions (1.4) and (1.5) are both far from their thermodynamic equilibrium. This demonstrates the stability of the CH_4 molecule in the gasification process. For the reaction (1.7) involving ethylene, the model did not allow reproducing the experimental concentration. This is probably due to the fact that ethylene is formed by other reactions than the one considered here (like cracking reactions).

Table 7 gives the heat and mechanical streams of the FICFB. The most important thermal streams are the one associated with the cooling of the syngas (q-1) and of the combustion gases (q-3). Part of this heat is available at relatively high temperatures and can consequently be used to produce mechanical work by combined heat and power.

Step 2: Methanation

Table 8 summarizes the assumptions made for each unit of the methanation step (figure 3). Table 9 gives the results obtained with this model. The inlet stream (*SYNG*) has the same composition as the gas mixture coming out from the wood gasification plant in Güssing. The efficiency of CO conversion into CH_4 (ratio between the amount of CH_4 produced and the maximum amount of CH_4 that can be stochiometrically produced using the inlet gas mixture) is 98.7% for the *Comflux* reactor and 96.7% for the whole methanation process. This difference is due to CH_4 losses in the water outlet stream (*H2OOUT2*).

Table 10 gives the heat and power streams obtained with the model of the *Comflux* process described above. It shows that an important amount of mechanical work is needed to compress the inlet gas mixture to the operation pressure in the *Comflux* reactor (0.27 kWh/Nm^3 of inlet gas mixture). A considerable amount of heat at 400°C released in the reactor could be used to produce high-pressure steam, which in turn could produce the mechanical power needed for pressurizing the gas inlet.

Step 3: Gas purification

To run the model corresponding to the separation of CH_4 from the *CH4DR2* stream, a CO_2/CH_4 selectivity of 35 [18] and different recovery ratios were chosen: 0.9 for membranes 1 and 2, and 0.6 for membrane 3. This high recovery ratio used for

*Corresponding author: FAX: 0041216933502, email: francois.marechal@epfl.ch

membrane 1 and 2 is justified by the fact that *(i)* the concentrations of CH_4 in the retention streams are not an important point as these streams do not leave the process, and by the fact that *(ii)* the CH_4 losses in the permeation stream must be avoided as the CH_4 contained in these streams is definitely lost, especially for membrane 2. On the other hand, a low recovery ratio was used for membrane 3 in order to have a sufficiently high concentration of CH_4 in the clean SNG stream. Finally, the other chemicals present in the inlet stream are partitioned between permeation and the retention according to what has been experimentally observed [18].

Table 12 summarizes the hypothesis used to run the model of the gas purification section. Table 13 presents the results obtained with this model and Table 14 gives the corresponding heat and power streams of the gas purification model.

This shows that this membrane process is suitable to purify a CO_2/CH_4 mixture efficiently. The clean gas produced meets the pipeline quality requirements (very low concentration of water and 96.1% of CH_4). Moreover, a high overall recovery ratio of methane is obtained (92%). Unfortunately a high mechanical energy consumption (0.125 kWh/Nm^3 treated) is calculated due to the compression of the permeation streams in the first two membranes (*M1M*) and (*M3M*).

Process integration

The compositions, the pressures, the temperatures, the LHVs and the flow rates of the gas mixtures at the end of each of the three steps of the whole process are presented in Table 15 which gives also the efficiencies, the thermal and the mechanical balances of each step. The following characteristics of the whole process can be calculated from this table:

- an overall carbon conversion efficiency of the process:

$$\eta_C = \frac{m_{C,out}}{m_{C,in}} = 34,7\%$$

  where $m_{C,in}$ and $m_{C,out}$ are the molar flow rates of carbon in the inlet, respectively outlet, streams;

- an overall thermal efficiency of 57.9% corresponding to the ratio of the LHV of the outlet SNG stream to the LHV_{daf} of the inlet wood stream;
- and a specific mechanical energy consumption of 627.9 kWh per ton of dry wood processed.

The thermal efficiency is very different for the three steps; the smallest is observed for the methanation without recycling *CH4RE* (71.0%). This can be explained by the highly exothermic reaction leading to heat losses during the process. The thermal efficiency of gasification is not very high either because a part of the biomass entering the process has to be burned in order to produce the heat needed by the gasification step.

The mechanical work consumption for the three steps is also very different, the highest being observed for the methanation. This is due to the negative stoichiometric coefficient variation of the reaction. Thus the compression of an important molar flow

*Corresponding author: FAX: 0041216933502, email: francois.marechal@epfl.ch

rate is needed to recover the heat of methanation at high temperature while keeping a good chemical conversion of the CO/H_2 mixture.

Based on the LHV of CH_4, the thermal output of the wood to methane process is 11.6 MW_{th} of pipeline quality methane compressed at 48bar. The energy balance of the system has been computed using process integration techniques. The excess of heat of the process could be usefully exploited by combined heat and power production in a steam expansion turbine. The amount of mechanical power produced with this excess of heat can be estimated by optimization [19] and visualized in the integrated composite curve [20] of the process (Figure 5):

- the dotted curve corresponds to the grand composite curve of the whole process: a segment from left to right means an excess of heat that needs to be extracted from the system; the temperature of this heat flux is given on the vertical axis.
- the dashed curve corresponds to the integrated steam system i.e. the steam production and usage integrated heat exchange with the hot and cold streams of the process.
- the rectangles correspond to the mechanical power generated by expansion of the high-pressure steam.

Hence, this graph shows first that a large excess of high temperature heat is available and secondly that the steam that can be generated from the surplus of heat available can be used to produce 585.9 kWh of mechanical energy per ton of dry wood. That leaves an input of only 42 kWh of mechanical energy per ton of dry wood needed to compress the generated SNG.

The same work has been undertaken with the second alternative of methanation, which consists in burning the methane recovered from the condensed water after a flash instead of being recycled. Table 11 compares the results obtained with the two alternatives. The heat recovered from this combustion allows producing more high-pressure steam and thus more mechanical energy than the first alternative (643.9 instead of 585.9kWh/t of wood processed). Moreover the mechanical energy consumption is less important when burning the methane. This is due to the fact that one recycling loop and one compressor have been eliminated. However, the thermal energy efficiency based on the LHV is higher when recycling the methane (57.9% instead of 54.1%). Thus a trade off must be found between a process that is energetically self-sufficient and one that exhibits a high thermal efficiency.

Finally, one should keep in mind that the energy needed to bring the wood from the forest to the plant situated in a range of 20 km and to process it into wood chips has not been taken into account in the power mechanical balance; this energy has been estimated to be 80 to 100kWh per ton of wood chips produced [21].

Conclusion

It has been observed that the FICFB model developed here has a behavior coherent with the FICFB pilot plant in Güssing. It can easily reproduce the experimental results just by varying the difference between the reaction temperature and that of the thermodynamic equilibrium for each reaction considered. This approach allows

*Corresponding author: FAX: 0041216933502, email: francois.marechal@epfl.ch

modeling a complete heat and mass balance of the system with the use of only a few experimental data.

The process configurations studied show an attractive efficiency of 57.9% based on LHV for the alternative recycling the methane recovered from the condensed water.

From the process integration curve, it has been shown that only about 7% of the mechanical energy needs should be imported from an external source, the remaining being obtained by converting the excess of heat produced on the spot.

Our study shows the importance of considering process design in order to quantify the overall conversion efficiency. It shows also the importance of the process integration that allows identifying ways of valorizing and optimizing the energy conversion efficiency. It is especially important for renewable energy production process, since renewable is very often very dilute; consequently, great care has to be taken in order to avoid investing more energy in the production process than what is produced.

References

[1] Global energy perspectives, IIASA-WEC, Cambridge University Press, 1998.

[2] BP statistical review of world energy, http://www.bp.com, 2003.

[3] Hersener P, Meier U, Energetisch nutzbares Biomassepotential in der Schweiz sowie Stand der Nutzung in ausgewählten EU-Staaten und den USA. Bundesamt für Energie. Bern, Switzerland, 1999.

[4] Friedli C, Biollaz S. Ecogaz, Projet-Bois méthane. EPFL-PSI, march 2003

[5] http://www.belsim.com

[6] Hofbauer H, Stoiber H. Veronik H. Gasification of organic material in a novel fluidization bed system. Proceedings of the first SCEJ symposium on fluidization, Tokyo, 1995; 291-299.

[7] Hofbauer H., Rauch R., Bosch K., Koch R., Aichernig C., Biomass, CHP plant Guessing – A success story. Available from http://www.ficfb.at.

[8] Gas production/Gas treating. In: Ullman's Encyclopedia of industrial chemistry. Online edition.

[9] Infelta P. Introductory thermodynamics. Boca Raton: Brown Walker Press, 2004.

[10] Schuster G, Löfller G, Weigl K, Hofbauer H. Bioressource Technology 2001; 77: 71-79.

[11] Reid RC, Prausnitz JM, Poling BE. The Properties of Gases and Liquids. New York: McGraw-Hill, 1987.

[12] Moeller FW, Robert H, Britz B. Methanation of coal gas for SNG. Hydrocarbon Processing, 1974

*Corresponding author: FAX: 0041216933502, email: francois.marechal@epfl.ch

[13] W.G. Bair WG, Leppin D, Lee AL. Design and operation of catalytic methanation in the hygas pilot plant. Paper presented at the American Chemical Society division of Fuel Chemistry, 1974.

[14] Flockenhaus C and Lommerzheim W. One stage shift-conversion and partial methanation process for upgrading synthesis gas to pipeline quality. Paper presented at the ninth Synthetic Pipeline Gas Symposium, 1977.

[15] Friedrichs G, Proplesch P, Wissman G, Lommerzheim W. Methanisierung von Kohlevergasungsgasen im Wirbelbett Pilot-Entwicklungsstufe. Duisburg: Thyssengas Gmbh, 1985.

[16] Seeman M, Biollaz S, Binkert P, Hottinger P, Marti T and Schneebeli J. Methanation of bio-syngas in a bench scale reactor. PSI Scientific report no. 23-24, 2003.

[17] Pilarczyk E, Henning KD, Knoblauch K. Ressources and conservation 1987; 14: 283-294

[18] Watanabe H. J. of membrane sc. 1999; 154: 121-126

[19] Marechal F., Kalitventzeff B. Applied Thermal Engineering. 2003; 23: 1763-1784

[20] Marechal F., Kalitventzeff B. Computers chem. Engng. 1996; 20: S225-S230

[21] Vuille F. Ecogas project, Life cycle assessment. GESTE Engineering SA, November 2003

*Corresponding author: FAX: 0041216933502, email: francois.marechal@epfl.ch

Notation:

$\alpha(A/B)$	Selectivity factor [-]
Cp_i	Heat capacity at constant pressure and at temperature T [J/mol/K]
d	Specific density of gas versus air [-]
$\Delta_r G_T$	Free enthalpy of reaction at temperature T [kJ/mol]
$\Delta_r H_T$	Enthalpy of reaction at temperature T [kJ/mol]
$\Delta_r H_T^0$	Standard enthalpy of reaction at temperature T [kJ/mol]
$\Delta_r S_T$	Entropy of reaction at temperature T [J/mol/K]
$\Delta_r S_T^0$	Standard entropy of reaction at temperature T [J/mol/K]
$\Delta_r Cp(T)$	Heat capacity of reaction at constant pressure and at temperature T [J/mol/K]
ΔT	Difference of temperature between the thermodynamic equilibrium temperature and the temperature corresponding to the composition of the gas mixture [K]
$\Delta\nu_r$	Variation of the stochiometric coefficient for the reaction *r* [-]
η_C	The overall carbon conversion efficiency [-]
FICFB	Fast Internally Circulating Fluidized Bed
$K_P(T)$	Thermodynamic equilibrium constant at a temperature T and a pressure P [$bar^{\Delta\nu}$]
K(T)	Thermodynamic equilibrium constant at a temperature T [-]
MWth	Mega watt thermal
LHV	Lower Heating Value [MJ/Nm^3]
LHVdaf	Lower Heating Value dry and free of ash [MJ/kg]
$m_{C,out}$	Molar flowrate of the carbon in the outlet stream [kmol/s]
$m_{C,in}$	Molar flowrate of the carbon in the intlet stream [kmol/s]
$\nu_{i,r}$	stochiometric coefficient of *i* in reaction *r* [-]
Nm3	Normal cubic meter [m^3]
P_i	partial pressure of i [-]
P_P, P_F	Pressure of the retentate and the feed stream respectively [bar]
SNG	Synthetic Natural Gas
θ_A	Recovery raio [-]
$W_{s,n}$	Wobbe index [kWh/Nm^3]
y_i	molar fraction of i [-]
y_{iR}, y_{iP}	Molar fraction of i in the retentate and the permeate stream respectively [-]

Figure 1 Schematic drawing of the FICFB reactor

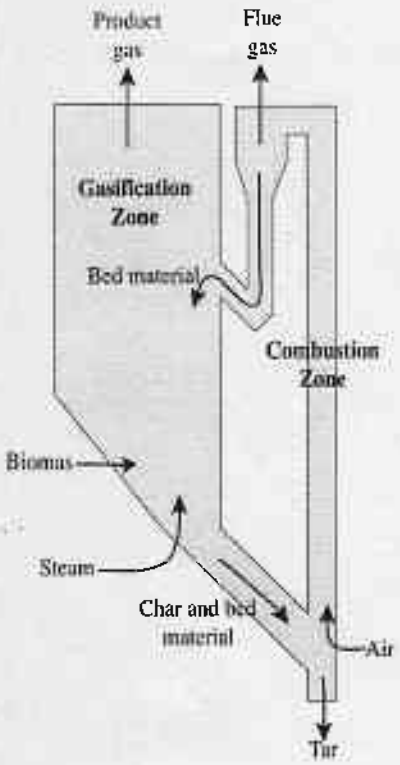

Figure 2 Flow diagram of the model of the Guessing demonstration plant

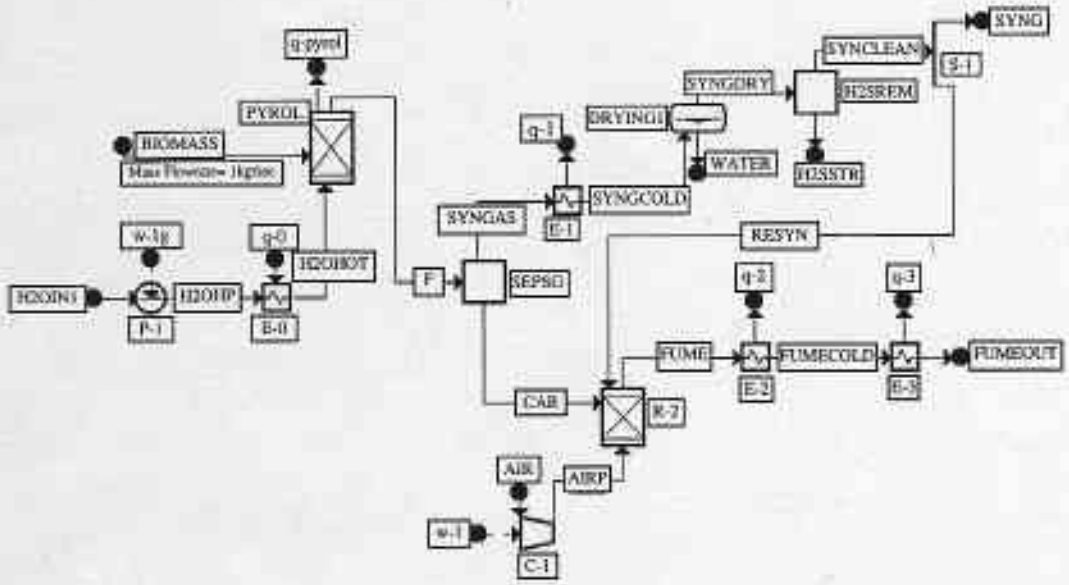

Figure 4 Flow diagram of the alternative one model

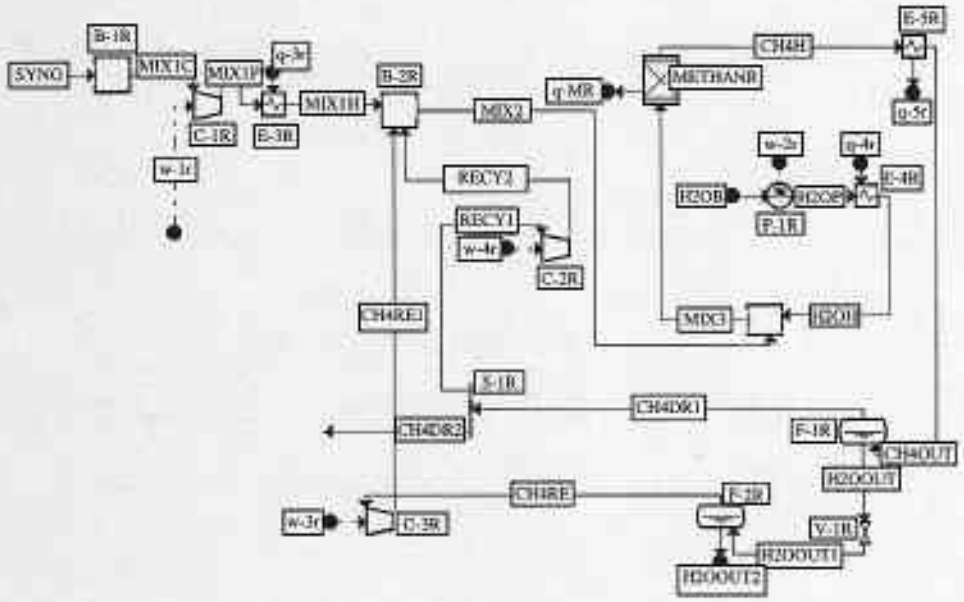

Figure 5 Process flow diagram of the membrane process used in this work

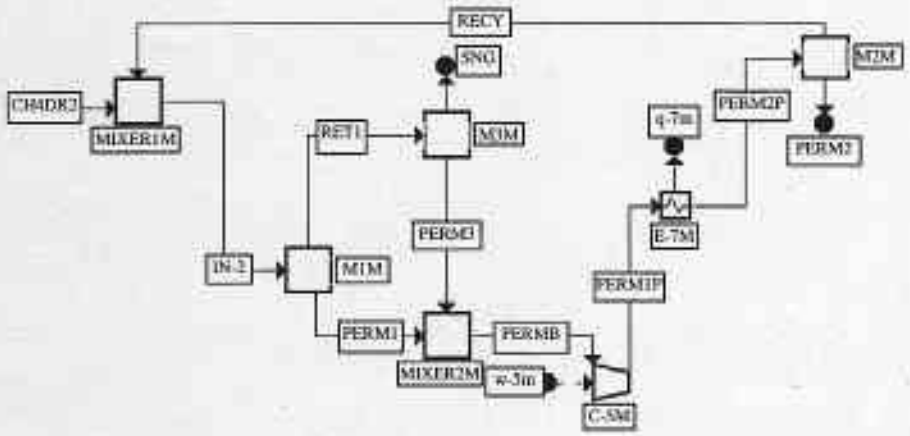

Figure 6 Integrated grand composite curve of the model of the whole process

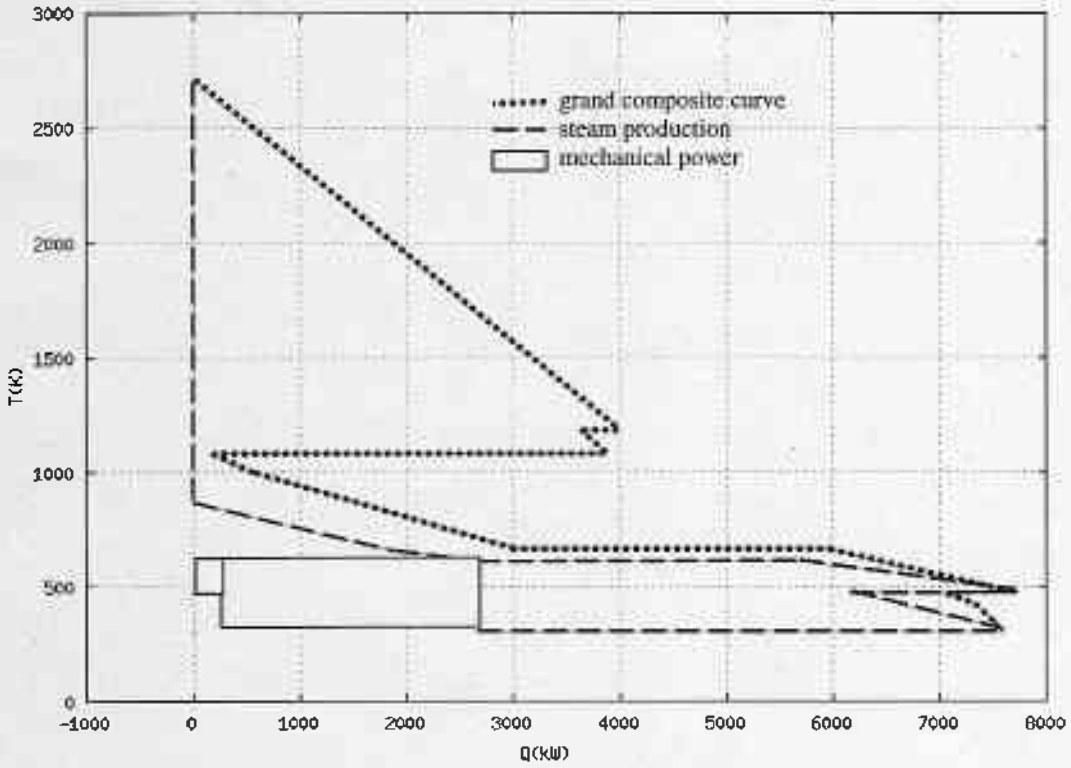

Table 1 Heterogeneous and homogeneous gasification reactions

	Reaction	*Name*	$^{*}\Delta_r H_T$ [kJ mol^{-1}]	$^{**}K_P$
(1.1)	$C(s) + CO_2 \Leftrightarrow 2CO$	Boudouard equilibrium	+ 172.54	14.1
(1.2)	$C(s) + 2H_2 \Leftrightarrow CH_4$	Hydrogenating gasification equilibrium	– 74.91	0.071
(1.3)	$C(s) + H_2O \Leftrightarrow CO + H_2$	Heterogeneous water-gas shift equilibrium	+ 131.38	7.5
(1.4)	$CH_4 + H_2O \Leftrightarrow CO + 3H_2$	Methane decomposition	+ 206.28	159.
(1.5)	$CO + H_2O \Leftrightarrow CO_2 + H_2$	Water gas shift equilibrium	– 41.16	1.02
(1.6)	$C_nH_m + nCO_2 \Leftrightarrow 2nCO + m/2H_2$	Boudouard equilibrium	-	-
(1.7)	$C_nH_m + 2nH_2O \Leftrightarrow nCO + (m/2+n)H_2$	Water gas shift equilibrium	-	-

* at 0°C, 1 atm ,
** at 800°C, 1 atm

Table 2 Methanation reactions

	Reaction	*Name*	$^*\Delta_r H_T$ [kJ mol^{-1}]	$^*\Delta_r S_T$ [J mol^{-1} K^{-1}]
(2.1)	$CO + 3H_2 \Leftrightarrow CH_4 + H_2O$	Reverse reforming reaction	− 218.4	− 243.4
(2.2)	$CO_2 + 4H_2 \Leftrightarrow CH_4 + 2H_2O$		− 179.9	− 206.7
(2.3)	$CO + H_2O \Leftrightarrow H_2 + CO_2$	Water gas shift reaction	− 37.5	− 36.7
(2.4)	$C_2H_4 + 2H_2O \Leftrightarrow 2CO + 4H_2$	Reforming reaction	+ 210.5	+ 190.7

* at 370°C, 1 atm

Table 3 Inlet stream compositions and flow rates

Inlet stream	*Pressure* [bar]	*Temperature* [°C]	*Flow rate* [kg scc^{-1}]	*Composition*
**BIOMASS*	1	25	1.1	30%C, 47%H, 22%O, 1.1E-4%N
H2OIN1	1	25	0.34	H_2O
AIR	1	25	**	Dry Air
H20B	1	25	***	H_2O

* Dry wood
** flow rate sufficient to have a stoichiometric composition in the combustion zone
*** flow rate equal to 0.1Nm^3 per Nm^3 of the flow rate of the inlet gas mixture *SYNG*

Table 4 Assumptions for each unit of the gasification process

Unit	*Function*	*Parameters / hypotheses*
P-1	Pump	Volumetric efficiency = 0.8 and pressure variation = 11 bar
E-0	Heat exchanger	No pressure drop and outlet temperature = 400°C
PYROL	Gasification reactor	No pressure drop, thermodynamic equilibrium, outlet temperature 800°C
SEPSG	Solid gas separator	No pressure drop and perfect separation
E-1	Heat exchanger	No pressure drop and outlet temperature = 25°C
DRYING1	Liq / Vap separator	No pressure drop
H2SREM	H_2S removal	No pressure drop and perfect removal of H_2S
S-1	Splitter	* No pressure drop and recycling rate 0.17
C-1	Compressor	Isentropic efficiency = 0.8 and pressure variation = 11 bar
R-2	Combust. reactor	Stoichiometric adiabatic combustion
E-2	Heat exchanger	No pressure drop and outlet temperature = temperature in the gasification zone + 100°C
E-3	Heat exchanger	No pressure drop and outlet temperature = 150°C

* 17% of the input stream is injected in the combustion zone (value from the pilot plant in Güssing)

Table 5 Compositions, pressures, temperatures and flow rates of the streams in the FICFB

Outlet stream	*P* [bar]	*T* [°C]	*Flow rate* [kg/sec]	*Composition* [mol%]								
				Coal	*Wood*	CH_4	*CO*	CO_2	H_2	H_2O	N_2	C_2H_4
*BIOMASS**	1	25	1	Dry wood (30%C, 47%H, 22%O, 1.1E^{-4} %N), LHV_{daf}=18.2MJ/kg								
**H2OIN1*[1]	1	25	0.31	0	0	0	0	0	0	100	0	0
**AIR*	1	25	3.31	Dry air (79% N_2 and 21% O_2)								
FUME												
Exp	1	150	3.58	0	0	0	0	13	0	20	62	0
Model	1	2442	3.75	0	0	0	0	10.0	0	20.9	62.6	0
RESYN												
Exp	1	25	0.18	0	0	11	25	22	37	0	3	2
Model	1	25	0.18	0	0	11.1	23.6	19.6	42.5	3.2	0	0
SYNG												
Exp	1	25	0.86	0	0	11	25	22	37	0	3	2
Model	1	25	0.86	0	0	11.1	23.6	19.6	42.5	3.2	0	0

* The experimental and model inlets have the same composition and flowrate (± experimental error)

[1] This stream contains the water from the wood stream (17 weight% of the wood inlet streams); the remaining water is used as gasifying agent.

Table 6 Difference between the measured temperature and the thermodynamic equilibrium temperature for each reaction occurring in the gasification zone

Reaction	ΔT [°C]	*Type of reaction*
(1.4)	– 224.4	endothermic
(1.5)	+ 39.8	exothermic
*(1.7)	-	endothermic

* with n = 2 and m = 4 (ethylene)

Table 7 Thermal and mechanical streams of the model FICFB plant after data reconciliation

Outlet stream	**Load* [kW]
q-0	1721.4
q-pyrol	1768.6
q-1	-3183.8
q-2	-1945.7
q-3	-3150.2
w-1g	0.76
w-1	960.5

* Counted positive if energy enters the process

Table 8 Assumptions for each unit of the CH4RE recycling methanation alternative

Unit	*Function*	*Parameters / hypotheses*
C-1R	Compressor	Isentropic efficiency = 0.8 and pressure variation = 59 bar
E-3R	Heat exchanger	No pressure drop and temperature in *MIX2* = 200°C
B-2R	Gas Mixer	No pressure drop for all inlet streams
B-3R	Mixer	No pressure drop for both inlet streams
P-1R	Water Pump	Volumetric efficiency = 0.8 and pressure variation = 59 bar
E-4R	Heat exchanger	No pressure drop and outlet temperature (*H2OH*) = 200°C
**METHANR*	Reactor	Thermodynamic equilibrium, pressure drop = 10 bar and outlet temperature = 400°C
E-5R	Heat exchanger	No pressure drop and outlet temperature = 30°C
F-1R	Liq / Vap separator	No pressure drop
V-1R	Valve	Adiabatic pressure drop important enough to recover 75% of the CH_4 in inlet stream in the vapor phase
F-2R	Liq / Vap separator	No pressure drop
C-3R	Compressor	Isentropic efficiency = 0.8 and pressure variation = 59 bar
S-1R	Splitter	No pressure drop and recycling rate 0.1 (vol/vol)
C-2R	Compressor	Isentropic efficiency = 0.8 and pressure variation = 59 bar

* The reactions considered here are the ones given in Table 2, except reaction (2.2) since it can be written as a combination of reaction (2.1) and (2.3)

Table 9 Compositions, pressures, temperatures, flow rates, and vapor fractions of the *Comflux* streams when recycling *CH4RE*

Outlet	*P* [bar]	*T* [°C]	*Vapor Fraction*	*Flow rate* [Nm^3/h]	*Composition* [mol%]						
					CH_4	CO	CO_2	H_2	H_2O	N_2	C_2H_4
SYNG	1	25	1	1000	11	25	22	37	0	3	2
H2OB	1	25	0	100	0	0	0	0	100	0	0
MIX2	60	200	1	1105	13.9	22.6	25	33.6	0	3.1	1.8
MIX3	60	142.4	0.97	1205	12.8	20.8	22.9	30.8	8.3	2.8	1.6
CH4H	50	400	1	899	37.4	0.2	42.4	0.9	15.3	3.8	0
CH4DR1	50	30	1	674	47.6	0.3	45.9	1.2	0.1	4.9	0
H2OOUT	50	30	0	225	6.9	0	31.9	0	60.9	0.3	0
CH4DR2	50	30	1	606.6	47.6	0.3	45.9	1.2	0.1	4.9	0
RECY1	50	30	1	67.4	47.6	0.3	45.9	1.2	0.1	4.9	0
H2OOUT2	19.3	15.7	0	188	2.1	0	25	0	72.9	0	0
CH4RE	19.3	15.7	1	37	31.2	0.1	66.8	0.2	0.1	1.6	0

Table 10 Thermal and mechanical streams of the *CH4RE* recycling alternative

Outlet stream	**Load* [kW]
q-3r	190.0
q-4r	16.6
q-5r	– 259.1
q-*MR*	– 335.0
w-1r	269.1
w-2r	0.12
w-3r	1.8
w-4r	0.5

* Counted positive if energy enters the process

Table 11 Comparison of the whole process results obtained with the two alternatives of methanation

	Whole Process (recycling CH4RE))	*Whole Process (without recycling CH4RE)*
Specific Mechanical Energy consumption [kWh/t]	627.9	619.2
Specific Mechanical Energy production [kWh/t]	585.9	643.9
Overall thermal efficiency [%]	57.9	54.1
Overall carbon conversion efficiency [%]	34.7	32.3

Table 12 Assumptions for each units of the gas purification

Unit	*Function*	*Parameters / hypotheses*
M1M	Membrane1	Recovery ratio of 0.9, pressure drop of 46 bar and 1 bar for the permeation and the retention streams respectively
M2M	Membrane2	Recovery ratio of 0.9, pressure drop of 46 bar and 1 bar for the permeation and the retention streams respectively
M3M	Membrane2	Recovery ratio of 0.6, pressure drop of 45 bar and 1 bar for the permeation and the retention streams respectively
MIXER2M	Gas mixer	No pressure drop for both streams
C-5M	Compressor	Isentropic efficiency = 0.8 and pressure variation = 46 bar
E-7M	Heat exchanger	No pressure drop, and Outlet temperature = 298 K

Table 13 Compositions, pressures, temperatures and flow rates of the model gas purification

Outlet stream	*P* [bar]	*T* [°C]	*Flow rate* [$Nm^3\ h^{-1}$]	*Composition* [mol%]						
				CH_4	CO	CO_2	H_2	H_2O	N_2	C_2H_4
CH4DR2	50	25	1000	47.6	0.3	45.9	1.2	0.1	4.9	0
in-2	50	25	1423	57.1	0.3	37.8	0.9	0.1	3.8	0
RET1	49	25	857.3	85.3	0.4	13.6	0	0.1	0.6	0
PERM1	4	25	565.7	14.4	0.2	74.5	2.1	0.1	8.7	0
SNG	49	25	456.2	96.1	0.6	3.1	0	0.1	0.1	0
PERM3	4	25	401.1	72.9	0.2	25.6	0	0.1	1.2	0
PERMB	4	25	966.8	38.7	0.2	54.2	1.2	0.1	5.6	0
RECY	50	25	423.0	79.5	0.4	18.7	0	0.1	1.3	0
PERM2	5	25	543.8	6.9	0.1	81.8	2.2	0.1	8.9	0

Table 14 Thermal and mechanical streams of the membrane process

Outlet stream	**Load* [kW]
q-7M	– 125.1
w-5M	125.0

* Counted positive if energy enters the process

Table 15 Compositions, pressures, temperatures and flow rates of the process streams

	Gasification	*Methanation*		*Gas purification*	
		Recycling	*No recycling*	*Recycling*	*No reclycling*
CO_2 [%vol.]	7.3	43.3	41.7	3.5	3.4
CO [%vol.]	37.6	0.2	0.2	0.4	0.4
H_2 [%vol.]	50.2	1.6	1.8	0	0
CH_4 [%vol.]	1.7	54.8	56.2	96.1	96.2
H_2O [%vol.]	3.2	0.1	0.1	0	0
N_2 [%vol.]	0	0	0	0	0
P [bar]	1	50	50	48	48
T [°C]	25	30	30	25	25
LHV [MJ Nm^{-3}]	10.769	19.814	20.351	34.425	34.483
Efficiency [%]	82.3	77.1	71.0	91.3	91.3
Mechanical power [kW]	593.6	1595.0	1583.74	298.0	274.50
Flow rate [Nm^3 h^{-1}]	5505.2	2305.7	2096.1	1211.9	1129.3